Virology 275, 238–243 (2000)
doi:10.1006/viro.2000.0489, available online at http://www.idealibrary.com on IDEAL®

RAPID COMMUNICATION

Nascent Synthesis of Leader Sequence-Containing Subgenomic mRNAs in Coronavirus Genome-Length Replicative Intermediate RNA

Tetsuya Mizutani, John F. Repass, and Shinji Makino[1]

Department of Microbiology and Immunology, The University of Texas Medical Branch at Galveston, Galveston, Texas 77555-1019

Received May 12, 2000; returned to author for revision June 6, 2000; accepted June 26, 2000

Infection with coronavirus results in the accumulation of genomic-sized mRNA and six to eight subgenomic mRNAs that make up a 3′ coterminal nested-set structure. Genome-length negative-strand RNA and subgenomic-length negative-strand RNAs, each of which corresponds to each of the subgenomic mRNAs, also accumulate in infected cells. The present study examined whether the genome-length negative-strand RNA serves as a template for subgenomic mRNA synthesis. Genome-length replicative intermediate (RI) RNA was purified by two-dimensional gel electrophoresis of intracellular RNAs from cells infected with mouse hepatitis virus. RNase A treatment of the purified genome-length RI resulted in the production of the genome-length replicative form RNA, indicating that the genome-length RI included genome-length template RNA. RNase protection assays using the purified genome-length RI and two probes, which corresponded to the 5′ 300-nt region of mRNA 6 and to the same region of mRNA 7, showed the presence of nascent leader sequence-containing subgenomic mRNAs in the genome-length RI. These data demonstrated that the genome-length negative-strand RNA serves as a template for subgenomic mRNA synthesis.

Coronavirus is an enveloped RNA virus containing a large positive-strand genomic RNA. Coronavirus-infected cells produce a genomic-sized mRNA, mRNA 1, and six to eight species of successively smaller subgenomic mRNAs, which form a 3′ coterminal nested-set structure (*1–3*). Characteristics of the unique coronavirus nested-set structure are that all the mRNAs are polyadenylated at the 3′-end; the messages are successively larger by one gene at the 5′-end with only the 5′-most gene on the polycistron being translated; and each has a 60- to 90-nt-long leader sequence at the 5′-end (*4–6*). The leader sequences are derived from the 5′-end of genomic RNA (the only place on the genome where they are encoded) and, by an unknown type of discontinuous synthesis (*7*), they join the 5′-ends of each of the messages at the intergenic regions. Infected cells also produce negative-strand genomic RNA and subgenomic RNAs, each of which corresponds to one mRNA species (*8*). These negative-strand RNAs contain a poly (U) sequence at the 5′-end and an anti-leader sequence at the 3′-end (*9*). Like coronaviruses, cells infected with arteriviruses produce a 3′ coterminal nested set of mRNAs with the leader sequence at the 5′-end of the mRNAs (*10*). Subgenomic negative-strand RNAs that correspond to each of the subgenomic mRNAs are also produced in arterivirus-infected cells. Coronaviruses and arteriviruses are classified under the newly established order Nidovirales; both viruses probably use similar transcription strategies.

One of the unsolved questions in nidovirus transcription is whether the template for subgenomic mRNAs is of genome length or subgenome length. Two major models have been proposed. One suggests that a genome-length negative-strand RNA serves as a template for all the mRNAs (*11*), while the other model proposes that each negative-strand subgenomic RNA is a unique template for synthesis of the correspondingly sized subgenomic mRNA (*8, 12–15*). A study using mouse hepatitis virus (MHV), a prototypic coronavirus, demonstrated that early in infection negative-strand genomic RNA, and not negative-strand subgenomic RNA, is the template for subgenomic mRNA synthesis (*16*); this study did not determine the template late in infection.

Here we describe whether MHV negative-strand genomic RNA is also the template for subgenomic mRNA synthesis late in infection. Previous studies of replicative intermediate (RI) RNAs in MHV-infected cells were based on the detection of two different types of RI RNAs: subgenomic RIs and genome-length RI. After a short pulse of radiolabeling, the subgenomic RIs (*13*) appear as six to seven discrete RNA bands when separated by using nondenaturing agarose gel electrophoresis. The polarity of these elongating RNAs in the subgenomic RIs has not

[1] To whom reprint requests should be addressed. Fax: (409) 772-5065. E-mail: shmakino@utmb.edu.

0042-6822/00 $35.00

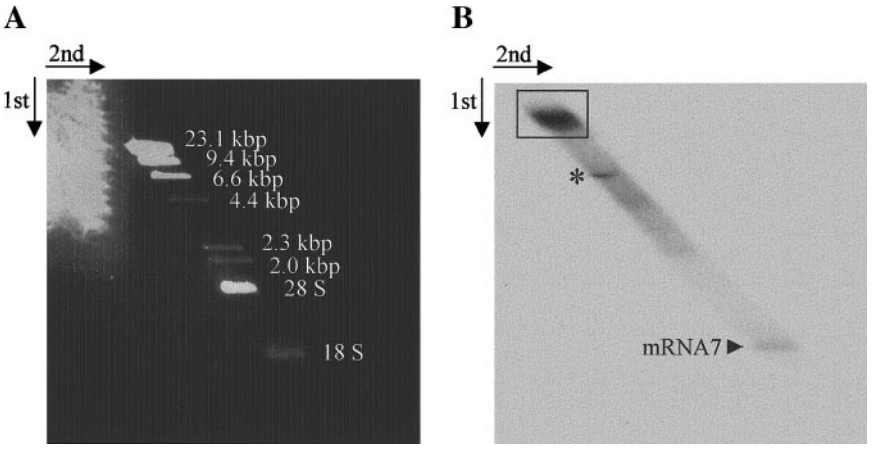

FIG. 1. Two-dimensional gel electrophoresis of the poly(A)-minus fraction of MHV-intracellular RNAs. ^{32}P-labled MHV-infected intacellular RNAs that did not bind to oligo-dT cellulose were mixed with lambda *Hin*dIII marker DNA fragments and separated on 0.8% nondenaturing two-dimensional gel electrophoresis. (A) Ethidium bromide staining of the gel after two-dimensional gel electrophoresis. Lambda *Hin*dIII marker DNA fragments and ribosomal RNAs (28S rRNA and 18S rRNA) are shown. (B) Autoradiogram of the two-dimensional gel. The box region containing genome-length RI was excised from the gel and used for further study. The asterisk is an artifact of the gel electrophoresis. A low level of mRNA 7, which was not completely removed by oligo-dT cellulose column chromatography, is also shown.

been identified. The genome-length RI RNA appears as a slowly migrating diffuse band on a nondenaturing electrophoretic gel (*11, 13*). RNase A treatment of the genome-length RI RNA results in the production of replicative-form (RF) RNA 1, which comigrates with mRNA 1 (*11, 13*), demonstrating that the nascent RNAs are elongating on genome-length template RNA in the genome-length RI. RNase T1 fingerprinting analysis showed that the majority of elongating RNAs in the genome-length RI are positive-sense (*11*), strongly indicating that the genome-length RI RNA must contain a genome-length negative-strand RNA template. Accordingly, if the negative-strand genome-length MHV RNA is a template for subgenomic mRNA synthesis, then all the subgenomic mRNAs are likely to be elongating in a genome-length RI RNA.

To test for the possibility that subgenomic mRNAs are elongating from the negative-strand genome-length MHV RNA in the genome-length RI RNA, we first purified genome-length RI RNA. DBT cells were infected with the A59 strain of MHV at a multiplicity of infection of 20; defective interfering RNAs were undetectable in this stock of MHV (*13*). The MHV RNAs were radiolabeled from 4 to 7 h postinfection (p.i.) with ^{32}Pi in the presence of actinomycin D as described previously (*17*). Intracellular RNA was extracted at 7 h p.i. using the Totally RNA kit (Ambion), treated with DNase I, and applied onto an oligo-dT cellulose chromatography column. The RNA fraction that did not bind to the oligo-dT cellulose was collected; this step lowered the amount of poly (A)-containing mature MHV mRNAs in the RNA preparation. Then the RNA sample was applied to a two-dimensional 0.8% TBE (89 mM Tris, 89 mM boric acid, 2 mM EDTA) agarose gel containing ethidium bromide (Fig. 1). We hoped that the two-dimensional gel electrophoresis would efficiently separate genome-length RI RNA from MHV subgenomic mRNAs. A strong diffuse radioactive RNA signal, which migrated slower than the 24-kbp-long lambda *Hin*dIII marker DNA fragment, was detected after two-dimensional gel electrophoresis. The gel region that migrated more slowly than the 24-kbp-long DNA fragment was excised carefully (Fig. 1). Based on a previous study of the genome-length RI (*13*), this region of the gel should contain the genome-length RI.

We further separated the RNA in the gel slices under different electrophoretic conditions to estimate the purity and the properties of the gel-purified genome-length RI. First we looked for contamination of subgenomic mRNAs in the gel-purified genome-length RI by processing the gel piece obtained after two-dimensional gel electrophoresis in a new, nondenaturing 0.8% TBE gel next to ^{32}P-labled MHV intracellular RNAs (Fig. 2A). Electrophoresis of the purified gel piece resulted in a diffuse slowly migrating signal whose migration pattern was similar to the published MHV genome-length RI RNA (*11, 13*). The purified gel pieces did not contain MHV mRNAs even after a long exposure of the gel (data not shown). Next we examined the production of the RF1 RNA after RNase A treatment of the purified gel pieces. The gel piece was treated with RNase A (0.33 μg/ml) in a buffer (233 mM NaCl, 3.3 mM Tris–HCl, pH 7.4, 10 mM EDTA) for 5 min at room temperature. After RNase A treatment, the gel piece was soaked in TBE buffer for 10 min at room temperature. Then the gel piece was placed into the well of a 0.8% TBE agarose gel and electrophoresed alongside labeled MHV intracellular RNAs (Fig. 2B), which resulted in a single band that roughly comigrated with mRNA 1. Subgenomic RF RNAs were not detected even after much longer exposure of the gel. The migration of this RNase-A-resistant band was very similar to that of the RF 1 RNA described previously (*11, 13*). We further

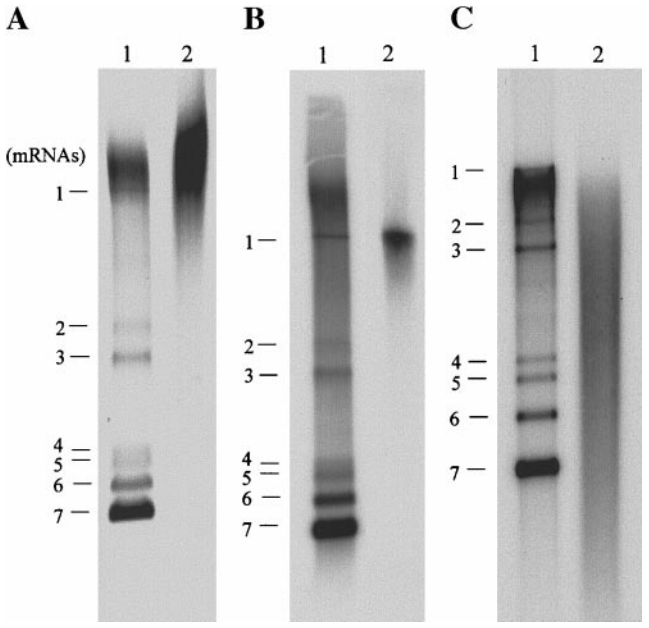

FIG. 2. Characterization of genome-length RI. (A) Nondenaturing agarose gel electrophoresis of purified gel pieces isolated after two-dimensional agarose gel electrophoresis (lane 2). Total intracellular RNAs from MHV-infected cells (lane 1). (B) Nondenaturing agarose gel electrophoresis of purified gel pieces after RNase A treatment (lane 2). Total intracellular RNAs from MHV-infected cells (lane 1). (C) Agarose gel electrophoresis of an RNA sample that was extracted from the purified gel pieces under the denaturing condition (lane 2). Total intracellular RNAs from MHV-infected cells (lane 1).

confirmed the presence of the genome-length RI RNA in the purified gel piece under denaturing gel electrophoresis. RNAs were extracted from the gel-purified gel pieces using the RNaid kit (BIO 101) and then separated using denaturing formaldehyde gel electrophoresis (Fig. 2C). We only detected a smeary signal, the size of which ranged from genomic in length to less than the size of mRNA 7; we saw no discrete MHV mRNAs. Incubation of genome-length RI at 65°C for 10 min and subsequent separation in a 0.8% TBE agarose gel also produced a similar smeary RNA signal (data not shown). We interpreted this absence of discrete mRNAs with the presence of a smeary signal to mean that the smear represented nascent RNAs that were elongating in genome-length RI. Other experiments showed poor recovery of RNA molecules larger than mRNA 3 from a gel, while recovery of small RNAs was excellent (unpublished data). This reduced efficiency of large RNA recovery from the first gel appears as a drop in signal above the size of mRNA 3 in the second separation (Fig. 1C). We repeated these experiments at least three times and obtained consistent results. We purified genome-length RI without contamination of any detectable level of MHV subgenomic mRNAs.

We used RNase protection assays to look for nascent subgenomic mRNAs containing the leader sequence in the genome-length RI. For these assays, an excess of two nonradiolabeled negative-sense RNA probes, one complementary to the 5′ 300-nt region of mRNA 6 (probe 1) and the other to the same region in mRNA 7 (probe 2), were independently mixed with heat-denatured ^{32}P-labeled purified genome-length RI. After hybridization and subsequent RNase A and RNase T1 treatment, RNase-resistant RNA fragments were detected on electrophoretic sequence gels. If leader-sequence-containing subgenomic mRNA 6 elongates on the genome-length RI, then the RNase protection assay using probe 1 and purified radiolabeled genome-length RI should produce a radiolabeled 300-nt-long RNA fragment (300-nt fragment) that corresponds to the 5′-end 300 nt of nascent mRNA 6 (see Fig. 3A). In addition, two RNA bands of approximately 70 and 240 nt long (240-nt fragment) should be detected, the former corresponding to the leader sequence of all the nascent mRNAs other than mRNA 6 and the latter to the 5′ 240-nt region of the mRNA 6 body sequence, which is found in nascent MHV mRNAs from 1 through 5. Similar results were expected for the RNase protection assay using probe 2; in this case a 300-nt-long radiolabeled RNA fragment should represent nascent leader-sequence-containing mRNA 7 (Fig. 3A). If only genome-length mRNA 1 elongates on genome-length RI, then the RNase protection assays using either probe should yield just a 70-nt-long band and a 240-nt-long band.

Two PCR products, each corresponding to the most 5′ 300 nt of mRNA 6 and mRNA 7, were cloned into a TA cloning vector (Invitrogen). Probe 1 and probe 2, the nonradiolabeled negative-strand RNA transcripts, were transcribed from cloned plasmids using the T7 mMESSAGE mMACHINE kit (Ambion). In a separate experiment, ^{32}P-labeled genome-length RI was prepared using two-dimensional gel electrophoresis as described above. RNAs were extracted from the gel pieces by using the RNaid kit, heat denatured at 65°C for 10 min, and quickly chilled on ice. Labeled RNAs were then applied to an oligo-dT cellulose chromatography column. We collected the RNA fraction that bound to the oligo-dT cellulose, the poly(A)-containing fraction, and the fraction that did not bind to the oligo-dT cellulose, the poly(A)-minus fraction. We assumed that the poly(A)-containing fraction included nascent poly(A)-containing mRNAs elongating in the genome-length RI and mature mRNAs that might be contaminating the purified genome-length RI preparation; and we assumed that the poly(A)-minus would include mostly nascent RNA molecules and possibly be contaminated with degraded mature MHV RNAs that lacked the poly(A) sequence. We separately mixed each of the RNA fractions with each of the probes and performed the RNase protection using the RiboQuant kit (Pharmingen), according to the manufacturer's instruction. After RNase A and T1 treatment, the samples were incubated with proteinase K and extracted using phenol–chloroform, and the RNAs were precipitated with etha-

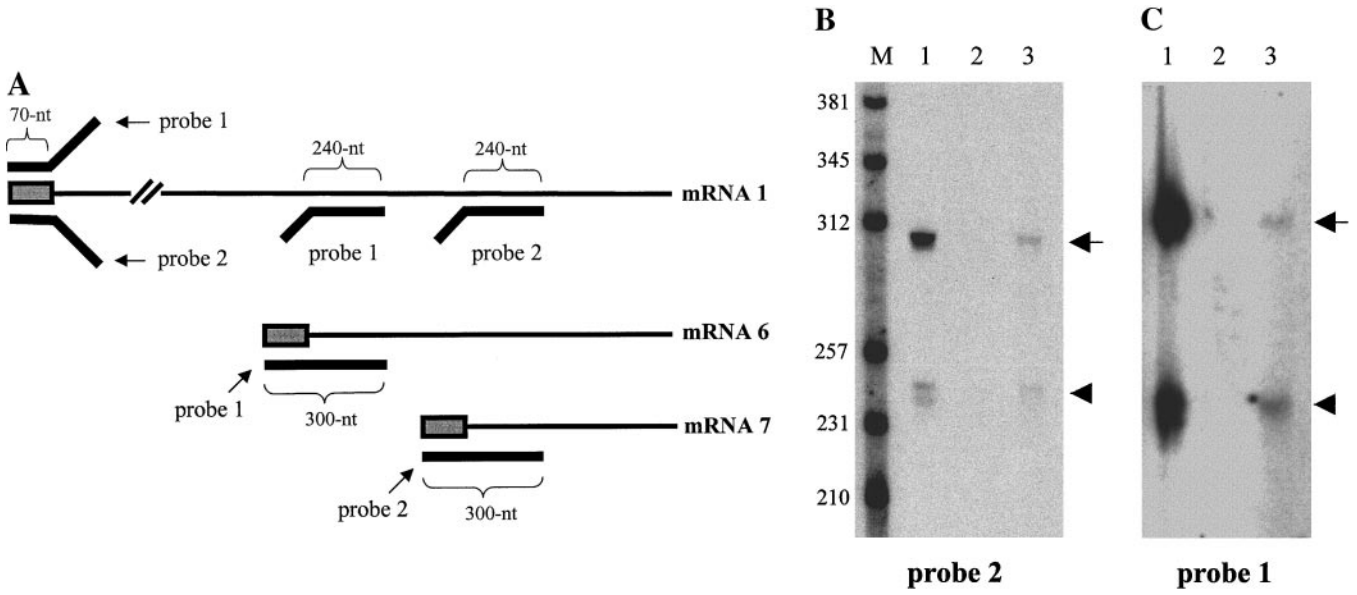

FIG. 3. RNase protection assay. (A) Schematic diagram of RNase protection assay. Binding sites of probe 1 and probe 2 to MHV mRNAs are shown. Shaded boxes represent the leader sequence. (B) RNase protection assay using total intracellular RNA from MHV-infected cells (lane 1), poly(A)-containing fraction of the purified genome-length RI (lane 2), and poly(A)-minus fraction of the purified genome-length RI (lane 3). RNA size marker (lane M). Probe 2 was used for RNase protection assay. The 300-nt fragment and the 240-nt fragment are indicated by an arrow and an arrowhead, respectively. (C) RNase protection assay using total intracellular RNA from MHV-infected cells (lane 1), poly(A)-containing fraction of the purified genome-length RI (lane 2), and poly(A)-minus fraction of the purified genome-length RI (lane 3). Probe 1 was used for RNase protection assay. The 300-nt fragment and the 240-nt fragment are indicated by an arrow and an arrowhead, respectively.

nol. Finally the RNAs were applied to a 6% polyacrylamide–urea gel. Control assays combining ^{32}P-labeled intracellular RNAs from MHV-infected cells with probe 2 and with probe 1 both yielded the 300- and the 240-nt fragments (Figs. 3B and 3C). Production of these two expected fragments demonstrated that this RNase protection assay could specifically distinguish mRNA 6 and mRNA 7 from intracellular viral mRNA species. The 240-nt fragment appeared as two closely migrating discrete bands (Fig. 3B); a shorter exposure of Fig. 3C, lane 1, also showed two closely migrating discrete bands making up the 240-nt fragment. The presence of sequence heterogeneity at the leader–body fusion site of MHV mRNA 6 (*18*) may be the reason for the two closely migrating 240-nt fragments in the RNase protection assay using probe 2. However, the origin of two 240-nt fragments in the RNase protection assay using probe 1 is unclear, because extensive sequence heterogeneity does not exist at the leader–body fusion site of mRNA 7 (*18*). It is possible that the RNase protection assay did not quantitatively reflect the actual amounts of individual intracellular viral mRNA species. The RNase protection assay using the poly(A)-minus fraction of the purified genome-length RI and probe 1 as well as the same RNA fraction and probe 2 both showed the 300-nt fragment and the 240-nt fragment (Figs. 3B and 3C). In contrast, neither the 300-nt nor the 240-nt fragment was detected when the poly(A)-containing fraction of the purified genome-length RI was used in combination with probe 2 or with probe 1. In three repeated experiments, we consistently detected 300- and 240-nt fragments using the poly(A)-minus fraction, while these bands were underdetectable or detected at a very low level using the poly(A)-containing fraction.

If the purified genome-length RI were contaminated with a large amount of mRNA 6 and mRNA 7, then we should have detected the 300-nt-long fragment in the poly(A)-containing fraction. The underdetectable levels of the 300-nt-long fragment and the 240-nt fragment in the poly(A)-containing fraction indicated that contamination with mRNAs was very low in the gel-purified genome-length RI. Consistent with RNase protection assay data, contamination of mature MHV subgenomic mRNAs in purified genome-length RI was at an underdetectable level when purified genome-length RI was separated by agarose gel electrophoresis (Fig. 2). In contrast, we clearly detected the 300-nt fragment in the poly(A)-minus fraction with either probe 1 or probe 2. As discussed above, this 300-nt fragment could be produced from nascent leader-sequence-containing mRNA 6 and mRNA 7 and/or from degraded MHV RNAs lacking the poly(A) sequence that might be residually present in the purified genome-length RI. Our preparation of MHV intracellular RNA showed minimal RNA degradation (Fig. 2A); therefore, in our RNase protection assays we think that the possibility that the 300-nt fragment was solely produced from contaminating degraded mRNAs is highly unlikely. More likely, the 300-nt fragment in the poly(A)-minus fraction was produced from nascent subgenomic mRNA 6 and mRNA 7, both of which contain the leader se-

quence. Theoretically, nascent leader-sequence-containing mRNAs 6 and 7, which are shorter than 300 nt in length, should produce a smeared RNA signal in the RNase protection assay. We could not detect the expected smeared RNA signals, so we supposed that the signal was too low to be detected under the present experimental conditions; in both autoradiograms, gels were exposed to X-ray films for 3 weeks, and further exposure had little effect on signal detection. RNase A treatment of the gel-purified genome-length RI produced RF 1 (Fig. 2B), and the RNase protection assay demonstrated the presence of nascent leader-sequence-containing subgenomic mRNAs in the genome-length RI. Apparently, leader-sequence-containing subgenomic mRNAs were produced from the genome-length negative-strand RNA in the genome-length RI. These data are consistent with the model of coronavirus discontinuous transcription (*7, 11*), which involves fusion of a leader sequence to every mRNA body during subgenomic mRNA synthesis.

The characteristics of the genome-length RI that we described here agree with earlier analyses of MHV genome-length RI (*11, 13*). Sawicki and Sawicki (*13*) described a slowly migrating genome-length RI during electrophoresis of intracellular RNA from MHV-infected cells in a nondenaturing gel. Their treatment of the gel fraction containing the genome-length RI with RNaseA gave mostly RF 1 and a low level of subgenome-length RF RNAs, RF 2 and RF 3; RF 2 and RF 3 may well have been due to the presence of contaminating subgenomic RIs in the genome-length RI preparation. Baric *et al.* also showed that genome-length RI RNA purified by Sepharose 2B-CL column chromatography migrates slowly on nondenaturing gels appearing as a smeared RNA and produces RF 1 after RNase A treatment (*11*). The authors compared RNase T1 fingerprinting patterns of column-purified genome-length RIs under two conditions. Under one condition the genome-length RI was digested with RNase T1 without denaturation and under the other condition the genome-length RI was digested after denaturation of RNA. They found that T1 spots corresponding to leader sequence and the leader–body fusion site for subgenomic mRNAs appear as strong spots in the sample treated under the nondenaturing condition (*11*). These data led the authors to propose that leader-sequence-containing subgenomic mRNAs elongate on genome-length RI. Although the previous study using the column-purified genome-length RI (*11*) and the present study used different experimental approaches to examine the nascent RNAs in the genome-length RI, the data from these two independent studies indicated that MHV genome-length negative-strand RNA is the template RNA for subgenomic mRNA synthesis. We showed that negative-strand genomic RNA is the template for subgenomic mRNA synthesis early in infection (*16*). Our new data strongly support the idea that negative-strand genomic RNA is a template for subgenomic mRNA synthesis throughout the infection.

RNase A treatment of MHV genome-length RI, in which nascent subgenomic mRNAs are elongating on a genome-length negative-strand RNA, resulted in RF 1. In contrast, alphaviruses, which produce a subgenomic mRNA that corresponds to the 3′-region of viral genome, produce three RF RNAs after RNase A treatment of alphavirus RI RNA; with this virus, genome RNA and subgenomic RNA elongate on a genome-length negative-strand RNA in its RI RNA (*19*). Why RNase A treatment of coronavirus genome-length RI produces RF 1 but not subgenome-length RFs is unknown.

Although the present study and the previous study (*16*) established that negative-strand genomic RNA is a template for MHV subgenomic mRNA synthesis throughout the infection, these studies do not eliminate the possibility that MHV subgenomic mRNA is also synthesized from subgenomic negative-strand template RNA late in infection. A number of studies aimed to test whether positive-strand RNA synthesis occurs using subgenomic negative-strand template RNA in cells infected with coronaviruses (*8, 12–14*) and with arterivirus (*15*), yet did not provide direct evidence of positive-strand RNA elongation from the subgenomic-length negative-strand template. Sawicki and Sawicki revealed the presence of subgenomic RIs in MHV-infected cells (*13*), and their data directly demonstrated elongation of nascent RNA on subgenomic-length template in infected cells, however, the polarity of the template RNA in the subgenomic RIs was not described. It is interesting to note that subgenomic RIs appear as discrete RNA bands that comigrate with subgenomic RFs, which were produced after RNase A treatment of subgenomic RIs (*13*); electrophoretic patterns of subgenomic RIs imply that subgenomic RI exists as a completely double-stranded form. Because RI RNAs that are efficiently synthesizing nascent RNA molecules appear as a diffuse RNA signal in nondenaturing gels, multiple nascent RNAs may not be produced in MHV subgenomic RIs. Instead, subgenomic RIs may exist as complete double-stranded RNAs, in which newly synthesized subgenome-length RNA of either polarity hybridizes with its subgenomic-length template RNA. Recently, Baric and Yount reported the kinetic radiolabeling analysis of MHV intracellular RNAs (*12*). They demonstrated that the incorporation of radioisotopes into a subgenomic RF RNA, RF 7, increases rapidly during 5-min pulse-labeling of MHV-infected cells; MHV RF RNAs were obtained after RNase treatment of ^{32}P-labeled MHV intracellular RNAs. The authors interpreted these data that the incorporation of radioisotopes into nascent positive-strand RNAs, which are elongating on subgenomic negative-strand template RNA in the subgenomic RI, is saturated quickly. They also showed the gradual increase of the RF 7 radioactivity after 5-min pulse-labeling, which they interpreted to represent the

synthesis of a constant and low level of subgenomic negative-strand RNA, which is used as a template for subgenomic mRNA synthesis. These interpretations of the data led the authors to claim that nascent positive-strand RNAs are elongating on subgenomic negative-strand template RNA in the subegenomic RI (*12*). However, their data can be interpreted differently such that subgenomic RIs are continuously produced efficiently in infected cells, whereas many of them are quickly degraded. Because subgenomic RIs may exist as complete double-stranded RNAs, subgenomic RIs can be an excellent interferon inducer; efficient accumulation of subgenomic RIs in infected cells may elicit the interferon activation pathway. It is not surprising that MHV has developed a mechanism that degrades most subgenomic RIs to inhibit double-strand RNA accumulation in infected cells. None of the published studies demonstrated the polarity of nascent RNAs elongating on subgenomic RIs in nidovirus-infected cells, hence it is possible that nascent negative-strand RNAs are elongating on subgenomic RIs. The data presented by Baric and Yount (*12*) do not exclude the possibility that subgenomic negative-strand RNA is elongating in the subgenomic RI RNA, which is unstable in infected cells.

ACKNOWLEDGMENT

This work was supported by Public Health Service Grant AI29984 from the National Institutes of Health.

REFERENCES

1. Lai, M. M., Brayton, P. R., Armen, R. C., Patton, C. D., Pugh, C., and Stohlman, S. A. (1981). Mouse hepatitis virus A59: mRNA structure and genetic localization of the sequence divergence from hepatotropic strain MHV-3. *J. Virol.* **39**(3), 823–834.
2. Leibowitz, J. L., Wilhelmsen, K. C., and Bond, C. W. (1981). The virus-specific intracellular RNA species of two murine coronaviruses: MHV-A59 and MHV-JHM. *Virology* **114**(1), 39–51.
3. Stern, D. F., and Kennedy, S. I. (1980). Coronavirus multiplication strategy. II. Mapping the avian infectious bronchitis virus intracellular RNA species to the genome. *J. Virol.* **36**(2), 440–449.
4. Lai, M. M., Patton, C. D., Baric, R. S., and Stohlman, S. A. (1983). Presence of leader sequences in the mRNA of mouse hepatitis virus. *J. Virol.* **46**(3), 1027–1033.
5. Lai, M. M., Baric, R. S., Brayton, P. R., and Stohlman, S. A. (1984). Characterization of leader RNA sequences on the virion and mRNAs of mouse hepatitis virus, a cytoplasmic RNA virus. *Proc. Natl. Acad. Sci. USA* **81**(12), 3626–3630.
6. Spaan, W., Delius, H., Skinner, M., Armstrong, J., Rottier, P., Smeekens, S., van der Zeijst, B. A., and Siddell, S. G. (1983). Coronavirus mRNA synthesis involves fusion of non-contiguous sequences. *EMBO J.* **2**(10), 1839–1844.
7. Jeong, Y. S., and Makino, S. (1994). Evidence for coronavirus discontinuous transcription. *J. Virol.* **68**(4), 2615–2623.
8. Sethna, P. B., Hung, S. L., and Brian, D. A. (1989). Coronavirus subgenomic minus-strand RNAs and the potential for mRNA replicons. *Proc. Natl. Acad. Sci. USA* **86**(14), 5626–5630.
9. Sethna, P. B., Hofmann, M. A., and Brian, D. A. (1991). Minus-strand copies of replicating coronavirus mRNAs contain antileaders. *J. Virol.* **65**(1), 320–325.
10. Snijder, E. J., and Meulenberg, J. J. (1998). The molecular biology of arteriviruses. *J. Gen. Virol.* **79**(Pt. 5), 961–979.
11. Baric, R. S., Stohlman, S. A., and Lai, M. M. (1983). Characterization of replicative intermediate RNA of mouse hepatitis virus: Presence of leader RNA sequences on nascent chains. *J. Virol.* **48**(3), 633–640.
12. Baric, R. S., and Yount, B. (2000). Subgenomic negative-strand RNA function during mouse hepatitis virus infection. *J. Virol.* **74**(9), 4039–4046.
13. Sawicki, S. G., and Sawicki, D. L. (1990). Coronavirus transcription: Subgenomic mouse hepatitis virus replicative intermediates function in RNA synthesis. *J. Virol.* **64**(3), 1050–1056.
14. Schaad, M. C., and Baric, R. S. (1994). Genetics of mouse hepatitis virus transcription: Evidence that subgenomic negative strands are functional templates. *J. Virol.* **68**(12), 8169–8179.
15. van Marle, G., Dobbe, J. C., Gultyaev, A. P., Luytjes, W., Spaan, W. J., and Snijder, E. J. (1999). Arterivirus discontinuous mRNA transcription is guided by base pairing between sense and antisense transcription-regulating sequences. *Proc. Natl. Acad. Sci. USA* **96**(21), 12056–12061.
16. An, S., Maeda, A., and Makino, S. (1998). Coronavirus transcription early in infection. *J. Virol.* **72**(11), 8517–8524.
17. Makino, S., Taguchi, F., Hirano, N., and Fujiwara, K. (1984). Analysis of genomic and intracellular viral RNAs of small plaque mutants of mouse hepatitis virus, JHM strain. *Virology* **139**(1), 138–151.
18. Makino, S., Soe, L. H., Shieh, C. K., and Lai, M. M. (1988). Discontinuous transcription generates heterogeneity at the leader fusion sites of coronavirus mRNAs. *J. Virol.* **62**(10), 3870–3873.
19. Simmons, D. T., and Strauss, J. H. (1972). Replication of Sindbis virus. II. Multiple forms of double-stranded RNA isolated from infected cells. *J. Mol. Biol.* **71**(3), 615–631.